Molecular constants of LiCl($X^1\Sigma^+$) and elastic collisions of two ground-state Cl and Li atoms at low and ultralow temperatures*

Zhu Zun-Lue(朱遵略)†, Zhang Xiao-Niu(张小妞), Kou Su-Hua(寇素华), Shi De-Heng(施德恒), and Sun Jin-Feng(孙金锋)

College of Physics and Information Engineering, Henan Normal University, Xinxiang 453007, *China*

(Received 11 March 2010; revised manuscript received 12 May 2010)

Interaction potentials for LiCl($X^1\Sigma^+$) are constructed by the highly accurate valence internally contracted multireference configuration interaction in combination with a number of large correlation-consistent basis sets, which are used to determine the spectroscopic parameters (D_0, D_e, R_e, ω_e, $\omega_e\chi_e$, B_e and α_e). The potentials obtained at the basis sets, i.e., aug-cc-pV5Z-JKFI for Cl and cc-pV5Z for Li, are selected to study the elastic collision properties of Li and Cl atoms at the impact energies from 1.0×10^{-12} to 1.0×10^{-4} a.u. The derived total elastic cross sections are very large and almost constant at ultralow temperatures, and their shapes are mainly dominated by the *s*-partial wave at very low impact energies. Only one shape resonance can be found in the total elastic cross sections over the present collision energy regime, which is rather strong and obviously broadened by the overlap contributions of the abundant resonances coming from various partial waves. Abundant resonances exist for the elastic partial-wave cross sections until $l = 22$ partial waves. The vibrational manifolds of the LiCl($X^1\Sigma^+$) molecule, which are predicted at the present level of theory and the basis sets cc-pV5Z for Li and the aug-cc-pV5Z-JKFI for Cl, should achieve much high accuracy due to the employment of the large correlation-consistent basis sets.

Keywords: atom–atom collision, shape resonance, interaction potential, molecular constant

PACC: 3520G, 3440

1. Introduction

It is well-known that the metal halides have important applications in various fields of sciences and technologies.[1] Among the metal halides, LiCl is one of the species which has received particular attention. Because, on the one hand, the monatomic lithium has been detected in a number of stars, substellar-mass objects[2] and in the interstellar medium.[3] Most of the lithium observed throughout the universe is believed to be formed during the era of Big Bang nucleosynthesis and in the galaxy through spallation reactions involving cosmic rays.[4] From these viewpoints, an understanding of abundance of lithium has crucial significance for theories of the early universe, interstellar processes, and galactic and stellar evolution;[5] on the other hand, the presence or the absence of Li I resonance line has played an important role in ascertaining whether the object is a brown dwarf. And the thermochemical equilibrium calculations of cool dwarf atmospheres suggest that the molecule should be the dominant Li-bearing gas over an extended domain of the temperature-pressure diagram. For these reasons, this molecule has been the subject of extensive investigations over the past several decades, both experimentally[6−15] and theoretically.[16−33]

In experiment, the earlier investigations on the LiCl were done by Klemperer and Rice[15] in 1957. Since then, the spectroscopic properties of the LiCl molecule have been widely studied by diode laser spectroscopy, infrared (IR) spectra, microwave spectra, flame photometry and so on.[6−14] In theory, the earlier *ab initio* calculations were reported by Matcha,[16] who evaluated the electronic structures and molecular properties in the self-consistent-field molecular-orbital approximation (SCF-LCAO-MO). Since then, a number of calculations[17−33] about the molecule have been made. Of particular interest is a comparison of these molecular parameters between experiment and theory. As a whole, these theories have presented a set of spectroscopic data, which are compared well with the experiments. However, the extracted spectroscopic properties from these experimental and theoretical investigations focus mainly on the spectro-

*Project supported by the National Natural Science Foundation of China (Grant Nos. 60777012 and 10874064), and the Program for Science and Technology Innovation Talents in Universities of Henan Province, China (Grant No. 2008HASTIT008).

†Corresponding author. E-mail: zl-zhu@henannu.edu.cn

© 2010 Chinese Physical Society and IOP Publishing Ltd

scopic parameters (D_e, R_e, ω_e, $\omega_e\chi_e$, α_e B_e and D_0). Little information about them is available from the literature dealing with its vibrational manifolds (vibrational levels, classical turning points, inertial rotation constants, etc.), which are very useful in the rovibrational transition calculations. Because there has been no accurate interaction potential up to date, no investigations can be found about the elastic scattering of Li and Cl atoms in the cold regime, since the elastic collision properties, such as the total and various partial-wave cross sections, are very sensitive to the details of interaction potential over an extended range of internuclear separations.

One of the main purposes at present is to construct the accurate interaction potential and provide the accurate molecular constants of the LiCl($X^1\Sigma^+$) molecule. Our calculations are carried out by the accurate valence internally contracted multireference configuration interaction (MRCI)[34,35] in combination with a number of correlation-consistent basis sets given by Dunning[36] and Peterson *et al.*[37,38] in the valence range. With the potentials obtained at the basis sets aug-cc-pV5Z-JKFI for Cl and cc-pV5Z for Li, the elastic collision properties of Li and Cl atoms are investigated in detail at impact energies from 1.0×10^{-12} to 1.0×10^{-4} a.u.. Atomic units are used throughout this paper unless otherwise specified.

2. Interaction potential

Here, we use the MRCI approach in combination with several large correlation-consistent basis sets to investigate the equilibrium internuclear distance R_e and harmonic frequency ω_e of the LiCl($X^1\Sigma^+$) molecule. Specifically in the calculations, the basis set for Li is cc-pV5Z at all times, whereas the basis sets for Cl are of aug-cc-pV5Z-JKFI (set 1), aug-cc-pV5Z-MP2F (set 2), aug-cc-pV6Z (set 3) and aug-cc-pV5Z (set 4). All the calculations are performed in the MOLPRO 2008.1 program package.[39] The R_e and the ω_e values determined at these basis sets are listed in Table 1.

Table 1. Spectroscopic parameter comparisons between available measurements and other theoretical values for LiCl($X^1\Sigma^+$) at the MRCI level of theory and four different groups of basis sets.

source		D_e/eV	R_e/nm	ω_e/cm^{-1}	$\omega_e\chi_e$/cm^{-1}	B_e/cm^{-1}	α_e/cm^{-1}	D_0/eV
this work	Set 1	4.8386	0.20327	659.24	4.5339	0.6982	0.00800	4.7979
	Set 2	4.7963	0.20332	652.12	4.5241	0.6978	0.00816	4.7560
	Set 3	4.7992	0.20366	637.25	4.5163	0.6955	0.00775	4.7598
	Set 4	4.7765	0.20348	649.71	4.9743	0.6967	0.00781	4.7364
Exp. [6]	(^{7}Li^{35}Cl)	4.8797	0.20207	643.31	4.501	0.7065	0.00801	4.84
Exp. [7]	(^{7}Li^{35}Cl)	—	—	642.955	4.47253	0.70652	0.00801	—
	(^{6}Li^{35}Cl)	—	—	686.068	5.0957	0.80444	0.00973	—
Exp. [8]	(^{7}Li^{35}Cl)	—	—	642.958	4.4751	0.70652	0.00801	—
	(^{6}Li^{35}Cl)	—	—	686.066	5.0953	0.80444	0.00973	—
Exp. [9]	(^{7}Li^{35}Cl)	—	0.20207	643.31	4.501	0.70652	0.00801	—
Exp. [10]	(^{7}Li^{35}Cl)	—	0.20207	643.31	4.501±0.019	0.70652	0.00801	—
	(^{6}Li^{35}Cl)	—	0.20207	686.23	5.096±0.019	0.80444	0.00973	—
Exp. [11]	(^{7}Li^{35}Cl)	—	0.20207	—	—	0.70653	0.00801	—
Exp. [12]		—	—	—	—	—	—	4.7917±0.13
Exp. [13]		—	—	—	—	—	—	4.8524
Exp. [14]		—	—	641±3	4.2±0.3	0.7053	—	4.85
Exp. [15]	(^{7}Li^{35}Cl)	—	0.2018	662	—	0.625	—	—
theory [16]	(^{7}Li^{35}Cl)	4.7348	0.20241	671.5	4.671	0.7042	—	—
theory [17]		—	0.1941	—	4.665	—	0.00759	—
theory [18]	(^{7}Li^{35}Cl)	—	0.20207	—	—	0.70652	—	—
theory [19]		—	—	—	4.641	—	0.00749	—
theory [20]	B–M	—	—	—	4.562	—	0.00725	4.5923
Hellmann	potential	—	—	—	4.755	—	0.00790	4.5446
theory [21]		—	0.2021	642.3	4.61	—	0.00758	—

Table 1. *continued*

source		D_e/eV	R_e/nm	ω_e/cm^{-1}	$\omega_e\chi_e$/cm^{-1}	B_e/cm^{-1}	α_e/cm^{-1}	D_0/eV
theory [22]	SCF	—	0.2036	650	—	—	—	4.79
	CI(SD)	—	0.2033	646	—	—	—	4.82
theory [23]	MVS	—	—	—	5.03	—	0.00676	—
	NR potential	—	—	—	4.61	—	0.00796	—
theory [24]		—	0.20207	—	—	—	—	—
theory [25]		—	—	712.9	3.84	—	0.00600	—
theory [26]		—	—	—	5.285	—	0.00924	—
theory [27]		—	0.2027	639.7	4.5	—	—	—
theory [28]		—	0.20200	650.2	—	0.71	—	—
theory [29]	(^{7}Li^{35}Cl)	4.6654	0.2037	638	4.47	0.695	0.00790	4.626
theory [30]		5.03	0.20278	644.09	4.44	—	—	4.99
theory [31]		4.962	0.20207	642.97	4.49	—	—	4.922
theory [32]	MRCI	4.5621	0.2035	639.4	—	—	—	4.523
first-order corrections		4.8275	0.209	636.2	—	—	—	4.788
theory [33]		4.83	0.20373	642	—	—	—	—

In general, the potential energy curve (PEC) calculations are carried out at intervals of 0.02 nm over the internuclear distance ranging from 0.08 to 2.5 nm. Only near the equilibrium position will the interval be of 0.005 nm. Over the present internuclear distance range for these basis sets, the obtained PECs are all smooth and completely convergent. These PECs are all fitted to the Murrell–Sorbie (M–S) function[40] with the least-squares fitting method. Here, the fitted values of dissociation energy D_e are presented in Table 1. And the fitting parameters a_i and D_e together with the R_e obtained at the set 1 are given in Table 2 for further convenient calculations.

Table 2. M–S APEF parameters for LiCl at the MRCI level of theory and set 1.

D_e/eV	R_e/nm	a_1/nm^{-1}	a_2/nm^{-2}	a_3/nm^{-3}	a_4/nm^{-4}	ΔE_{RMSE}/eV
4.8386	0.20327	1.73347	0.574413	0.519450	0.051762	0.008748

Now, we determine the spectroscopy parameters (B_e, α_e, $\omega_e\chi_e$ and D_0) as per the APEFs fitted here using the Rydberg–Klein–Rees (RKR) equations.[41,42] The calculated results are also presented in Table 1. In order to conveniently make a comparison, we also collect the available measurements[6−15] and other theoretical results[16−33] in this Table.

A number of theoretical calculations on the spectroscopic parameters have been done in the past several decades. Early in 1967, Matcha[16] made the investigations on the electronic structures and the molecular properties of the LiCl within the SCF-LCAO-MO framework using the double zeta basis set. From Table 1, it is easy to find that their D_e and $\omega_e\chi_e$ values greatly deviate from the experiments.[6−12] Afterwards, the spectroscopic properties of the LiCl molecule have been widely studied. However, most calculations were not complete.[17−28,30−33] For example, the important spectroscopic constant, D_e, was not included in these investigations.[17−28] In Refs. [30]–[33] only D_e was determined but other two important spectroscopic constants, B_e and α_e, were not evaluated. Although in Ref. [29] almost all the spectroscopic parameter (D_0, D_e, R_e, ω_e, $\omega_e\chi_e$, B_e and α_e) were calculated, and their D_e and D_0 are far from the available experiments.[6,12]

From Table 1, one can find that almost all the R_e and ω_e values at these basis sets are in good agreement with the available experiments.[6,9−11] And other spectroscopic parameters, D_e, B_e, $\omega_e\chi_e$, α_e and D_0, which are reproduced from the APEFs fitted here, also perfectly conform with the measurements,[6−15] especially for the results calculated using the set 1. For example, at the set 1, the deviations of the D_0, D_e, R_e, $\omega_e\chi_e$, B_e and α_e from the corresponding experiments[6] are only 0.87%, 0.84%, 0.59%, 0.73%, 1.17% and 0.13%, respectively. These prove that the present APEF given in Table 2 is accurate and reliable. And these also show that the present spectroscopic properties are more accurate and complete as a whole when com-

pared with previous theoretical calculations.[16−33]

In order to obtain more accurate D_e, R_e and ω_e, we take into consideration the effects on these spectroscopic parameters by the relativistic corrections at these basis sets. The results obtained by the non-relativistic (NR) calculations and by the standard second-order Douglas–Kroll–Hess Hamiltonian (DKH2) corrections are collected in Table 3. To be clear at a glance, the deviations from the NR results by the DKH2 corrections are also listed in this table.

Table 3. Spectroscopic parameter (R_e, ω_e and D_e) comparisons obtained from experiments for LiCl($X^1\Sigma^+$) by NR and DKH2 corrections at the MRCI level of theory.

basis sets	property	NR	DKH2	relativistic corrections
Set 1:	R_e/nm	0.20328	0.20317	–0.00011
Cl-aug-cc-pV5Z-JKFI	ω_e /cm^{-1}	659.24	748.78	89.54
Li-cc-pV5Z	D_e /eV	4.8386	4.8259	–0.0127
Set 2:	R_e/nm	0.20332	0.20324	–0.0008
Cl-aug-cc-pV5Z-MP2F	ω_e /cm^{-1}	652.12	664.69	12.57
Li-cc-pV5Z	D_e /eV	4.7963	4.7846	–0.0117
Set 3:	R_e/nm	0.20366	0.20360	–0.00006
Cl-aug-cc-pV6Z	ω_e /cm^{-1}	637.25	637.12	-0.13
Li-cc-pV5Z	D_e /eV	4.7992	4.7863	–0.0129
Set 4:	R_e/nm	0.20348	0.20341	–0.0007
Cl-aug-cc-pV5Z	ω_e /cm^{-1}	649.71	675.03	25.32
Li-cc-pV5Z	D_e /eV	4.7765	4.7634	–0.0131
Exp.[6]	R_e = 0.20207 nm; ω_e = 643.31 cm^{-1};D_e = 4.8797 eV			

In Table 3, it is not difficult to find that the DKH2 corrections make the D_e small, thus further deviating from the available experimental results, when compared with the present one at all these basis sets. That is to say, for all these basis sets, the D_e obtained at the non-relativistic calculations is in better agreement with the experiments[6] than the ones corrected by the relativistic effects. As to the ω_e, the DKH2 corrections also make it worse when compared with the non-relativistic calculations. Only the R_e becomes slightly closer to the measurements[6] under the DKH2 corrections. According to these, we think that the results obtained at the non-relativistic calculations are in better accordance with the experiments than those obtained at the DKH2 corrections as a whole. Therefore, we employ the PEC obtained at the non-relativistic calculations for further investigations.

The more stringent way to compare the *ab initio* results with the measurements is to attempt to reproduce the RKR data: the vibrational levels, classical turning points and inertial rotation constants. Since only in that way can it be clearly demonstrated whether the present APEF accurately describes the LiCl($X^1\Sigma^+$) interaction potential. To predict the vibrational states of the LiCl($X^1\Sigma^+$) molecule, we must solve the radial Schrödinger equation of nuclear motion in the adiabatic approximation,

$$\left[-\frac{\hbar^2}{2\mu}\frac{\mathrm{d}^2}{\mathrm{d}r^2}+\frac{\hbar^2}{2\mu r^2}J(J+1)+V(r)\right]\Psi_{\nu,J}(r) = E_{\nu,J}\Psi_{\nu,J}(r), \quad (1)$$

where $V(r)$ is the rotationless APEF given in Table 2; r is the internuclear distance between two atoms, Li and Cl; μ is the reduced mass of the LiCl($X^1\Sigma^+$) molecule; ν and J are the vibrational and the rotational quantum numbers, respectively; $E_{\nu,J}$ and $\Psi_{\nu,J}(r)$ are the eigenvalue and the eigenfunction of the potential $J(J+1)\cdot\hbar^2/2\mu r^2+V(r)$, respectively. The rotational sublevel of a given vibrational level is represented by the following power series:

$$\begin{aligned} E_{\nu,J} = {} & G(\nu)+B_\nu[J(J+1)]-D_\nu[J(J+1)]^2 \\ & +H_\nu[J(J+1)]^3+L_\nu[J(J+1)]^4 \\ & +M_\nu[J(J+1)]^5+N_\nu[J(J+1)]^6 \\ & +O_\nu[J(J+1)]^7, \end{aligned} \quad (2)$$

where $G(\nu)$ is the vibrational level; B_ν is the inertial rotation constant; D_ν, H_ν, L_ν, M_ν, N_ν and O_ν are the centrifugal distortion constants. By solving Eq. (1) with the Numerov method,[43] we can obtain a total of 126 vibrational states for the LiCl($X^1\Sigma^+$) molecule when the rotational quantum number J is set to equal zero ($J=0$). For each vibrational state,

1 vibrational level, 1 inertial rotation constant and 6 centrifugal distortion constants are obtained. Here, due to the length limitation of the paper, we present only the first 32 vibrational levels, classical turning points and inertial rotation constants in Table 4.

Table 4. Vibrational levels, classical turning points and inertial rotation constants for the first 31 vibrational states of LiCl($X^1\Sigma^+$) when $J = 0$ at the MRCI level of theory.

ν	$G(\nu)/\mathrm{cm}^{-1}$	$R_{\min}/\mathrm{nm}$	$R_{\max}/\mathrm{nm}$	B_ν/cm^{-1}	ν	$G(\nu)/\mathrm{cm}^{-1}$	$R_{\min}/\mathrm{nm}$	$R_{\max}/\mathrm{nm}$	B_ν/cm^{-1}
0	323.262	0.19439	0.21337	0.6988690	16	9531.003	0.16459	0.28439	0.5828563
1	962.390	0.18856	0.22165	0.6909050	17	10042.546	0.16381	0.28786	0.5764869
2	1592.174	0.18485	0.22783	0.6830230	18	10547.592	0.16306	0.29130	0.5702227
3	2212.795	0.18200	0.23317	0.6752268	19	11046.292	0.16235	0.29472	0.5640623
4	2824.438	0.17966	0.23802	0.6675198	20	11538.796	0.16167	0.29812	0.5580045
5	3427.288	0.17765	0.24256	0.6599053	21	12025.247	0.16102	0.30149	0.5520474
6	4021.532	0.17588	0.24687	0.6523862	22	12505.783	0.16040	0.30485	0.5461894
7	4607.355	0.17430	0.25101	0.6449651	23	12980.538	0.15980	0.30818	0.5404284
8	5184.944	0.17287	0.25502	0.6376443	24	13449.641	0.15922	0.31151	0.5347623
9	5754.483	0.17156	0.25892	0.6304259	25	13913.214	0.15866	0.31482	0.5291887
10	6316.156	0.17035	0.26274	0.6233114	26	14371.375	0.15813	0.31812	0.5237052
11	6870.145	0.16923	0.26647	0.6163022	27	14824.237	0.15761	0.32140	0.5183095
12	7416.629	0.16819	0.27015	0.6093991	28	15271.908	0.15711	0.32468	0.5129989
13	7955.785	0.16721	0.27377	0.6026029	29	15714.491	0.15662	0.32794	0.5077707
14	8487.786	0.16629	0.27735	0.5959138	30	16152.084	0.15615	0.33120	0.5026225
15	9012.804	0.16542	0.28089	0.5893317	31	16584.780	0.15570	0.33446	0.4975514

To our surprise, only the theoretical literature[16] reported the B_ν values for the first three levels. In order to keep clarity of Table 4, we separately list these results in Table 5. It is easy to find that the B_ν results in Table 4 are in excellent agreement with these theoretical results.[16] The differences between them are only 0.233%, 0.302% and 0.390% for $\nu = 0$, 1 and 2, respectively.

Table 5. Other theoretical B_ν results for LiCl($X^1\Sigma^+$) when $J = 0$.

source	B_0/cm^{-1}	B_1/cm^{-1}	B_2/cm^{-1}
theory[16]	0.7005	0.6930	0.6857

Unfortunately, to the best of our knowledge, no experiments can be found in the literature about the vibrational levels, classical turning points and inertial rotation constants. Thus, we cannot make any comparison between them. But according to the high-quality fitting of the APEF, the good accordance between the present spectroscopic parameters and the available measurements[6−15] and the excellent agreement of the inertial rotation constants between the present results and previous theoretical results,[16] we have reasons to believe that the results collected in Table 4 are accurate and reliable. Furthermore, we can conclude that the APEF given in Table 2 can well describe the interaction potential of the LiCl ($X^1\Sigma^+$) molecule.

3. Total and partial-wave elastic cross sections

Now we use the APEF given in Table 2 to investigate the total and the various partial-wave cross sections of collisions between Li and Cl atoms at low and ultralow temperatures. To calculate the total and the various partial-wave cross sections, we must derive the radial solution u_l of the lth partial-wave equation. In order to determine the radial solution u_l of the lth partial-wave equation, we must solve the following radial Schrödinger equation:[44]

$$\frac{\mathrm{d}^2 u_l}{\mathrm{d}r^2} + \left[k^2 - \frac{2\mu V(r)}{\hbar^2} - \frac{l(l+1)}{r^2}\right] u_l(r) = 0, \quad (3)$$

where $V(r)$ is the APEF given in Table 2, μ is the reduced mass of the colliding system, and k is the wave number given in terms of the energy E of relative motion, i.e., $k^2 = 2\mu E/\hbar^2$. After u_l is obtained, the

scattering phase shift δ_l of the lth partial wave can be derived from[45]

$$\tan\delta_l = \frac{-2\mu}{\hbar^2 k}\int_0^\infty \mathrm{J}_l(kr)V(r)u_l(r)\mathrm{d}r, \qquad (4)$$

where J_l is the spherical Bessel function, and l is equal to 0, 1, 2, ... The elastic cross section of lth partial wave, $\sigma_l(E)$, is defined as[44−46]

$$\sigma_l(E) = \frac{4\pi}{k^2}\cdot(2l+1)\sin^2\delta_l. \qquad (5)$$

Then, the total elastic cross section, $\sigma_{\mathrm{T}}(E)$, can be computed from

$$\sigma_{\mathrm{T}}(E) = \sum_{l=0}^{\infty}\sigma_l(E) = \frac{4\pi}{k^2}\sum_{l=0}^{\infty}(2l+1)\sin^2\delta_l. \qquad (6)$$

Using the APEF given in Table 2, Eq. (3) can be numerically solved by the Numerov method[42] with the automatic step-size selection. The values of partial-wave phase shift δ_l of the elastic collisions between Li and Cl atoms at low and ultralow temperatures are evaluated from Eq. (4) when two atoms approach each other along the LiCl($\mathrm{X}^1\Sigma^+$) interaction potential. Various partial-wave cross sections and the total elastic cross sections are computed according to Eqs. (5) and (6) at the impact energies from 1.0×10^{-12} to 1.0×10^{-4} a.u. The collision energy dependence of the total elastic cross sections at low and ultralow temperatures is depicted in Fig. 1. And the collision energy dependences of elastic cross sections for some partial waves are presented in Figs. 2–6, respectively.

Figure 1 demonstrates that the total elastic cross sections vary with the collision energy of two atoms. Obviously, the total cross sections of elastic scattering of the ground-state Li and Cl atoms are very large and almost constant at ultralow temperatures. From the variation with energy of the elastic cross section of individual partial wave, we can see that the s-wave cross sections are significant but the remaining partial-wave elastic cross sections are very small when the impact energy is below 10^{-7} a.u. Especially when the energy is lower than 10^{-8} a.u., only the s wave has substantial contributions to the total cross sections. Therefore, the total elastic cross sections are dominated by the s-wave scattering over this impact energy regime. With energy increasing, the s-wave cross sections tend to decrease, but the decrease is quickly overcome by the higher partial-wave contributions. Particularly when the impact energy is higher than 10^{-6} a.u., the significance of the higher partial waves becomes greatly prominent. Therefore, as shown in Fig. 1, a very strong and broad shape resonance appears due to the contributions from the abundant resonances of the higher partial waves.

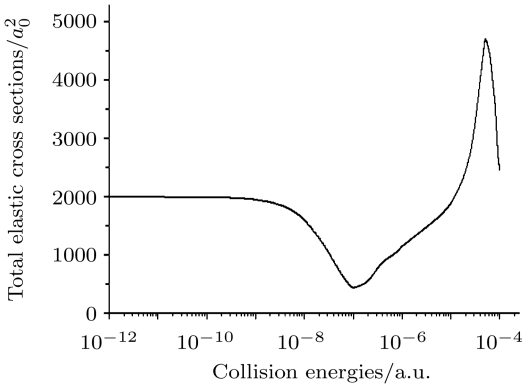


Fig. 1. Total elastic cross section versus collision energy for scattering along the interaction potential of the LiCl ground state.

In order to find out all the resonant structures in the total cross sections, we perform the careful calculations with very small energy steps. As a result, we discover only one. Careful investigations show that the resonant energy is 5.083×10^{-6} a.u. From Fig. 1, we can clearly see that this shape resonance is rather strong and broad. From Figs. 2–6 and Table 6, we know that numerous resonances exist in various partial-wave cross sections. It is the overlap contributions of these partial-wave cross sections that make the total elastic cross sections rather strong and broad.

Four resonant peaks exist in Fig. 2. Of these shape resonances, only one is strong. Their resonant energies from low to high are 7.805×10^{6}, 3.705×10^{5}, 6.130×10^{-5} and 9.290×10^{-5} a.u., respectively. Obviously, these peaks are all drowned in the strong total elastic cross sections.

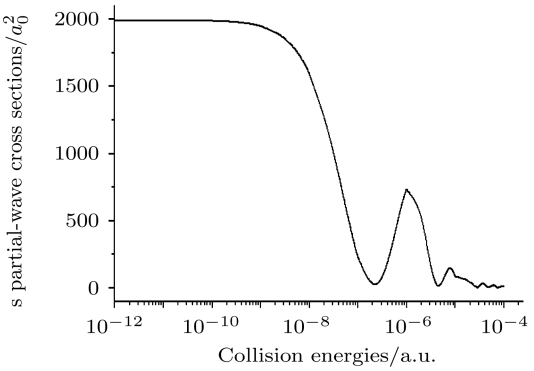


Fig. 2. s partial-wave cross section versus collision energy for scattering along the interaction potential of the LiCl ground state.

Figure 3 presents the collision energy dependence of elastic cross section for p-partial wave. As depicted in Fig. 3, one can instantly see that two relatively strong and four relatively weak shape resonances exist in this partial wave. Accurate calculations show that their resonant energies from low to high are 3.290×10^{7}, 3.325×10^{6}, 1.000×10^{-5}, 2.680×10^{-5}, 4.755×10^{-5} and 7.535×10^{-5} a.u., respectively. Here, a strong shape resonance comes out at impact energy 3.290×10^{7}. This resonance is the only one that appears below 10^{-6} a.u. energy region for various partial-wave cross sections of this LiCl($X^1\Sigma^+$) molecule.

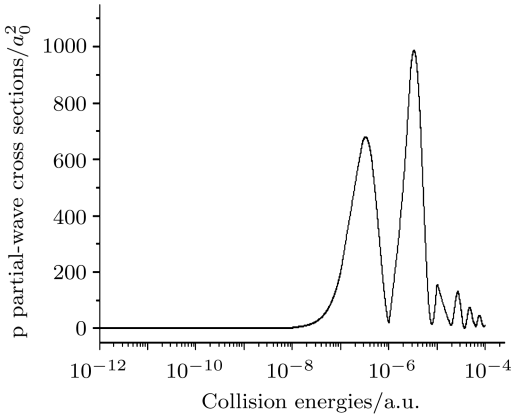


Fig. 3. p partial-wave cross section versus collision energy for scattering along the interaction potential of the LiCl ground state.

Six resonant structures exist in Fig. 4. At low temperatures, with energy increasing, the first sharp resonance appears and its resonant energy is 1.000×10^{6} a.u. Subsequently, the second resonant peak occurs. This peak is the strongest one among these six resonances in the d partial wave cross sections and its resonant energy is 5.900×10^{6} a.u. The third peak is also strong when compared with the rest. For the last four resonances, the resonant energies from low to high are 1.755×10^{5}, 3.500×10^{5}, 5.905×10^{5} and 9.045×10^{5} a.u., respectively. In similarity to Fig. 3, these six resonances also become strong and wide resonant peaks in the total elastic cross section.

In similarities to Figs. 3 and 4, luxuriant resonances can also be found in Figs. 5 and 6. In Fig. 5, five peaks exist and their resonant energies are 2.209×10^{6}, 9.099×10^{6}, 2.345×10^{5}, 4.395×10^{5} and 7.145×10^{5} a.u., respectively. In Fig. 6, five resonances appear and their resonant energies from low to high are 3.685×10^{6}, 1.000×10^{5}, 3.000×10^{5}, 5.370×10^{5} and 8.470×10^{5} a.u., respectively. Because the total elastic cross sections are too strong and broad, these resonances are all buried in oblivion as shown in Fig. 1.

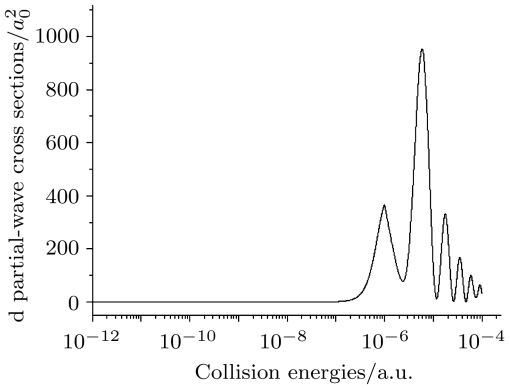


Fig. 4. d partial-wave cross section versus collision energy for scattering along the interaction potential of the LiCl ground state.

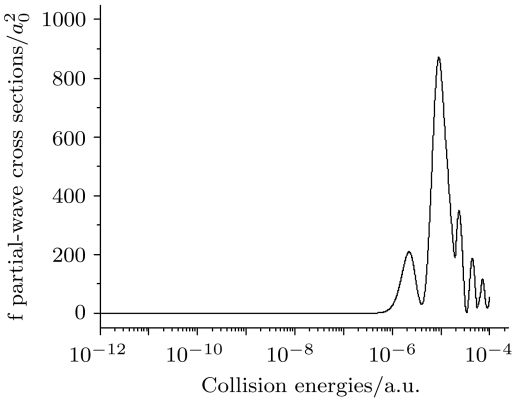


Fig. 5. f partial-wave cross section versus collision energy for scattering along the interaction potential of the LiCl ground state.

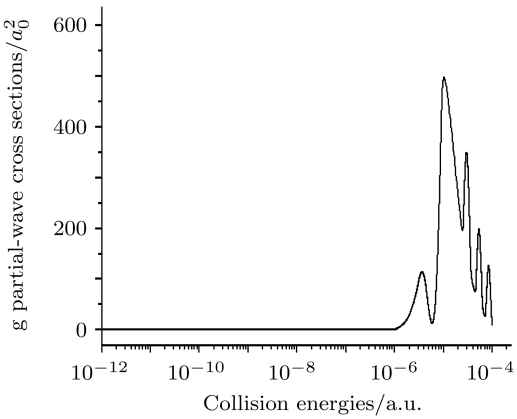


Fig. 6. g partial-wave cross section versus collision energy for scattering along the interaction potential of the LiCl ground state.

There are still a number of resonant structures from $l = 5$ to $l = 22$ partial-wave cross sections. Because of the length limitation of the paper, we may not give their collision energy dependences of the total elastic cross sections. Instead of giving plots, we

tabulate these shape resonant energies and their corresponding partial-wave elastic cross sections as shown in Table 6. Since the total elastic cross sections are too strong, similar to the circumstances shown in Figs. 2–6, these resonances are also completely drowned in Fig. 1. When the partial-wave number is higher than 22, no resonances exist. And when the partial-wave number is higher than 29, their contributions to the total elastic cross sections can be neglected.

Table 6. Shape resonant energies and their corresponding partial-wave elastic cross sections for scattering of Li and Cl along the PEC of the LiCl($X^1\Sigma^+$) molecule.

Partial waves	Resonant energies (partial-wave elastic cross sections)
5	5.44×10^{-6}(57.84); 1.65×10^{-5}(768.51); 3.72×10^{-5}(348.04); 6.42×10^{-5}(202.34)
6	7.39×10^{-6}(26.12); 2.09×10^{-5}(720.36); 4.49×10^{-5}(340.89); 7.54×10^{-5}(203.78)
7	9.38×10^{-6}(9.67); 2.56×10^{-5}(679.68); 5.32×10^{-5}(332.50); 8.72×10^{-5}(203.33)
8	3.06×10^{-5}(645.56); 6.19×10^{-5}(323.81)
9	3.58×10^{-5}(617.17); 7.11×10^{-5}(315.31)
10	4.11×10^{-5}(593.91); 8.07×10^{-5}(307.26)
11	4.65×10^{-5}(575.38); 9.06×10^{-5}(299.80)
12	5.17×10^{-5}(561.50)
13	5.66×10^{-5}(552.64)
14	6.08×10^{-5}(550.17)
15	4.09×10^{-5}(898.56)
16	5.16×10^{-5}(752.39)
17	6.44×10^{-5}(611.12)
18	7.68×10^{-5}(443.72)
19	8.76×10^{-5}(268.69)
21	6.47×10^{-5}(771.37)
22	8.12×10^{-5}(658.57)

We have studied the elastic collisions between several ground-state atoms at low and ultralow temperatures using the present theoretical method.[47−49] The results are in excellent agreement with the experiments. Thus, the present method should be reliable. Since the interaction potential obtained here is reliable and accurate, we should believe that the total and the various elastic cross sections calculated in the present paper are reliable and accurate though no experimental and theoretical results about the elastic collisions between two Cl and Li atoms at low and ultralow temperatures can be found for direct comparison. These results are expected to be detected experimentally and to be examined theoretically in the near future.

4. Conclusions

The accurate interaction potentials have been constructed and the spectroscopic parameters have been determined for the LiCl($X^1\Sigma^+$) molecule by using the MRCI theory and several large correlation-consistent basis sets. The APEF obtained at the basis sets, cc-pV5Z for Li and aug-cc-pV5Z-JKFI for Cl, is used to predict the vibrational state. By numerically solving the radial Schrödinger equation of nuclear motion with the Numerov method, a total of 126 vibrational states are found. For each vibrational state, the vibrational level, the classical turning points, the inertial rotation constant and the centrifugal distortion constant are also calculated when $J = 0$. The total and the various elastic cross sections of collision between Li and Cl atoms are investigated for the first time when they approach each other along the LiCl($X^1\Sigma^+$) interaction potential. Only one shape resonance is found in the total elastic cross sections over the present collision energy regime, which is rather strong and obviously broadened by the resonant contributions coming from various partial waves. Abundant resonances exist at the elastic partial-wave cross sections until $l = 22$ partial waves. It is the overlap contributions of these partial-wave cross sections that make the total elastic cross sections rather strong

and broad. No resonances exist when the partial-wave number is higher than 22. And the contributions to the total elastic cross sections can be neglected when the partial-wave number is higher than 29. Analyses show that the shape of the total elastic cross section is mainly dominated by the s-partial wave at very low temperatures.

References

[1] Hargittai M 2000 *Chem. Rev.* **100** 2233

[2] Kirkpatrick J D, Reid I N, Liebert J, Cutri R M, Nelson B, Beichman C A, Dahn C C, Monet D G, Gizis J E and Skrutskie M F 1999 *Astrophys. J.* **519** 802

[3] Knauth D C, Federman S R, Lambert D L and Crane P 2000 *Nature* **405** 656

[4] Hosseini B H, Weck P F, Sadeghpour H R, Kirby K and Stancil P C 2009 *J. Chem. Phys.* **130** 054308

[5] Korn A J, Grundahl F, Richard O, Barklem P S, Mashonkina L, Collet R, Piskunov N and Gustafsson B 2006 *Nature* **442** 657

[6] Huber K P and Herzberg G 1979 *Molecular Spectra and Molecular Structure*, Vol.4, *Constants of Diatomic Molecules* (New York: Van Nostrand Reinhold) p378

[7] Jones H and Lindenmayer J 1987 *Chem. Phys. Lett.* **135** 189

[8] Thompson G A, Maki A G, Olson Wm B and Weber A 1987 *J. Mol. Spectrosc.* **124** 130

[9] Gilbert T L 1968 *Second Midwest Chemistry Conference*, WIS-TCI-302. These involved data were abstracted by Brumer P and Karplus M in *J. Chem. Phys.* **58** (1973) 3903

[10] Pearson E F and Gordy W 1969 *Phys. Rev.* **177** 52

[11] Lide D R, Cahill P and Gold L P 1964 *J. Chem. Phys.* **40** 156

[12] Bulewicz E M, Phillips L F and Sugden T M 1961 *Trans. Faraday Soc.* **57** 921

[13] Brewer L and Brackett E 1961 *Chem. Rev.* **61** 425

[14] Klemperer W, Norris W G, Büchler A and Emslie A G 1960 *J. Chem. Phys.* **33** 1534 and references herein

[15] Klemperer W and Rice S A 1957 *J. Chem. Phys.* **26** 618

[16] Matcha R L 1967 *J. Chem. Phys.* **47** 4595

[17] Redington R L 1970 *J. Phys. Chem.* **74** 181

[18] Watson J K G 1973 *J. Mol. Spectrosc.* **45** 99

[19] Finn E J 1975 *J. Chem. Phys.* **62** 1842

[20] Shanker J, Agrawal H B and Agrawal G G 1980 *J. Chem. Phys.* **73** 4056

[21] Kumar M, Kaur A J and Shanker J 1986 *J. Chem. Phys.* **84** 5735

[22] Langhoff S R, Bauschlicher C W and Partridge H 1986 *J. Chem. Phys.* **84** 1687

[23] Kumar M and Shanker J 1992 *J. Chem. Phys.* **96** 5289

[24] Ogilvie J F 1992 *Spectrosc. Lett.* **25** 1341

[25] Dotelli G, Lombardi E and Jansen L 1994 *J. Mol. Struct.* (*Theochem*) **306** 117

[26] Hati S, Datta B and Datta D 1996 *J. Phys. Chem.* **100** 19808

[27] Bacskay G B and Buckingham A D 1997 *Mol. Phys.* **91** 391

[28] Gutsev G L, Nooijen M and Bartlett R J 1997 *Chem. Phys. Lett.* **276** 13

[29] Seth M, Npointner M P, Bowmaker G A and Schwerdtfeger P 1999 *Mol. Phys.* **96** 1767

[30] Weck P F, Kirby K and Stancil P C 2004 *J. Chem. Phys.* **120** 4216

[31] Weck P F, Schweitzer A, Kirby K, Hauschildt P H and Stancil P C 2004 *Astrophys. J.* **613** 567

[32] Lee D K, Lee Y S, Hagebaum-Reignier D and Jeung G H 2006 *Chem. Phys.* **327** 406

[33] Mintz B, Wilson A K and Bagus P S 2009 *Chem. Phys. Lett.* **468** 286

[34] Werner H J and Knowles P J 1988 *J. Chem. Phys.* **89** 5803

[35] Knowles P J and Werner H J 1988 *Chem. Phys. Lett.* **145** 514

[36] Dunning T H 1989 *J. Chem. Phys.* **90** 1007

[37] Peterson K A, Woon D E and Dunning T H 1994 *J. Chem. Phys.* **100** 7410

[38] Peterson K A, Kendall R A and Dunning T H 1993 *J. Phys. Chem.* **99** 1930

[39] Werner H J, Knowles P J, Lindh R, Manby F R, Schütz M, Celani P, Korona T, Mitrushenkov A, Rauhut G, Adler T B, Amos R D, Bernhardsson A, Berning A, Cooper D L, Deegan M J O, Dobbyn A J, Eckert F, Goll E, Hampel C, Hetzer G, Hrenar T, Knizia G, Köppl C, Liu Y, Lloyd A W, Mata R A, May A J, McNicholas S J, Meyer W, Mura M E, Nicklass A, Palmieri P, Pflüger K, Pitzer R, Reiher M, Schumann U, Stoll H, Stone A J, Tarroni R, Thorsteinsson T, Wang M and Wolf A 2008 *MOLPRO*, version 2008.1, a package of *ab initio* programs

[40] Murrell J N, Carter S, Farantos S C, Huxley P and Varandas J C 1984 *Molecular Potential Energy Functions* (Chichester: John Wiley & Sons) p9

[41] Zhang X N, Shi D H, Zhang J P, Zhu J L and Sun J F 2010 *Chin. Phys.* B **19** 053401

[42] Shi D H, Zhang J P Liu Y F Sun J F and Zhu Z L 2009 *Int. J. Quantum. Chem.* **109** 1159

[43] González J L M Q and Thompson D 1997 *Comput. Phys.* **11** 514

[44] Côté R and Dalgarno A 1994 *Phys. Rev.* A **50** 4827

[45] Côté R, Dalgarno A and Jamieson M J 1994 *Phys. Rev.* A **50** 399

[46] Jamieson M J, Dalgarno A and Yukich J N 1992 *Phys. Rev.* A **46** 6956

[47] Zhang X N, Shi D H, Sun J F and Zhu Z L 2010 *Chin. Phys.* B **19** 013501

[48] Zhang X N, Shi D H, Zhang J P, Zhu Z L and Sun J F 2010 *Chin. Phys.* B **19** 053401

[49] Shi D H, Zhang J P, Sun J F, Liu Y F and Zhu Z L 2009 *Acta Phys. Sin.* **58** 7646 (in Chinese)